THE JOURNAL OF BIOLOGICAL CHEMISTRY VOL. 289, NO. 10, pp. 6604–6618, March 7, 2014


# Transcriptional Factors Smad1 and Smad9 Act Redundantly to Mediate Zebrafish Ventral Specification Downstream of Smad5*

Received for publication, January 11, 2014, and in revised form, January 29, 2014 Published, JBC Papers in Press, January 31, 2014, DOI 10.1074/jbc.M114.549758

**Chang-Yong Wei (魏昌勇)[‡§], Hou-Peng Wang (王厚鹏)[‡], Zuo-Yan Zhu (朱作言)[‡], and Yong-Hua Sun (孙永华)[‡1]**

*From the [‡]State Key Laboratory of Freshwater Ecology and Biotechnology, Institute of Hydrobiology, Chinese Academy of Sciences, 7 Donghu South Road, Wuhan 430072, China and the [§]University of the Chinese Academy of Sciences, Beijing 100049, China*

**Background:** Ventral specification is regulated by Smad1-, Smad5-, and/or Smad9-mediated bone morphogenetic protein (BMP) signaling.
**Results:** Double knockdown instead of single knockdown of *smad1* and *smad9* induces dorsalization, which cannot be rescued by *smad5* overexpression.
**Conclusion:** *smad1* and *smad9* act redundantly and downstream of *smad5* to mediate ventral specification.
**Significance:** The regulation network and cooperative roles of BMP R-Smads in early development are clarified.

**Bone morphogenetic proteins (BMPs) are multifunctional growth factors that play crucial roles during embryonic development and cell fate determination. Nuclear transduction of BMP signals requires the receptor type Smad proteins, Smad1, Smad5, and Smad9. However, how these Smad proteins cooperate *in vivo* to regulate various developmental processes is largely unknown. In zebrafish, it was widely believed that the maternally expressed *smad5* is essential for dorso-ventral (DV) patterning, and the zygotically transcribed *smad1* is not required for normal DV axis establishment. In the present study, we have identified zygotically expressed *smad9*, which cooperates with *smad1* downstream of *smad5*, to mediate zebrafish early DV patterning in a functional redundant manner. Although knockdown of *smad1* or *smad9* alone does not lead to visible dorsalization, double knockdown strongly dorsalizes zebrafish embryos, which cannot be efficiently rescued by *smad5* overexpression, whereas the dorsalization induced by *smad5* knockdown can be fully rescued by overexpression of *smad1* or *smad9*. We have further revealed that the transcription initiations of *smad1* and *smad9* are repressed by each other, that they are direct transcriptional targets of Smad5, and that *smad9*, like *smad1*, is required for myelopoiesis. In conclusion, our study uncovers that *smad1* and *smad9* act redundantly to each other downstream of *smad5* to mediate ventral specification and to regulate embryonic myelopoiesis.**

The transforming growth factor $\beta$ (TGF-$\beta$) family plays crucial roles in regulating diverse cellular and developmental processes, such as cell proliferation, differentiation, and migration and embryonic pattern formation. Signaling by members of the TGF-$\beta$ superfamily is transduced by Smad proteins, which are classified into three subfamilies: the receptor-regulated Smads (R-Smads),[2] the common mediator Smad (Co-Smad), and the inhibitory Smad (I-Smad) (1, 2). Among the R-Smad subfamily members, Smad2 and Smad3 mediate the TGF-$\beta$/activin pathways, whereas Smad1, Smad5, and Smad9 (also known as Smad8) transduce the bone morphogenetic protein (BMP) pathway (3, 4). BMPs consist of the largest subgroup within the TGF-$\beta$ superfamily. In early development of vertebrates, BMPs are required for the dorso-ventral (DV) axis formation during gastrulation and embryonic hematopoiesis (5, 6).

The three BMP R-Smads share an extremely high degree of homology, and their cellular function is transducing BMP signaling. Consistent with this notion, much evidence shows that they have overlapping functions during development. In zebrafish and *Xenopus*, misexpression of either *smad1* or *smad5* in the embryo induces ventral fates (7–9). In chicken, the functions of *Smad1* and *Smad5* are largely interchangeable during spinal cord neurogenesis (10). In mammals, *Smad1*, *Smad5*, and *Smad9* are believed to function redundantly in transducing the anti-Mullerian hormone signal and mediating regression of the Mullerian duct in males (11). In addition, *Smad1* and *Smad5* function redundantly in the apical ectodermal ridge and ventral ectoderm (12), in endochondral bone formation and in controlling tumor cell migration to distant locations (13, 14).

However, accumulating evidence suggests that BMP R-Smads are not always interchangeable in development. In zebrafish, *smad1* and *smad5* were believed to have distinct functions in regulating early DV patterning, and the previous results from loss-of-function and gain-of-function studies even led to controversial conclusions. For instance, *smad5* mutants (such as $sbn^{-/-}$) or morphants are strongly dorsalized (15–18),

* This work was supported by China 973 Project Grants 2010CB126306 and 2012CB944504, the National Science Fund for Excellent Young Scholars of the National Natural Science Foundation of China (NSFC) Grant 31222052, NSFC Grant 30771100, and FEBL Grant 2011FBZ23 (to Y. H. S.).
[1] To whom correspondence should be addressed. Tel.: 8627-6878-0235; E-mail: yhsun@ihb.ac.cn.

[2] The abbreviations used are: R-Smad, Co-Smad, and I-Smad, receptor-regulated, common mediator, and inhibitory Smad, respectively; BMP, bone morphogenetic protein; DV, dorso-ventral; MO, morpholino; CHX, cycloheximide; hpf, hours postfertilization; WISH, whole-mount *in situ* hybridization; DIG, digoxigenin; MBT, midblastula transition; SBE, Smad-binding element.

demonstrating that *smad5* is essentially required for early DV patterning. In contrast, effective loss of function of *smad1* does not cause any phenotype of dorsalization (19), although overexpression of *smad1* strongly ventralizes zebrafish embryos as does *smad5* overexpression (9). This implies that *smad1* itself is not essential for zebrafish DV axis establishment. On the other hand, overexpression of *smad1* rather than *smad5* leads to complete rescue of zebrafish mutants of *bmp2b* (9), suggesting that *smad1* might be a direct mediator for ventral specification in the *bmp2b* null condition. Ectopic overexpression of *smad5* just after midblastula transition can rescue the $sbn^{-/-}$ dorsalized embryos, whereas no rescue effects could be observed if the exogenous *smad5* is forced to express only during gastrulation (17). Besides, the expression of non-neuroectoderm-specific *gata2* is mediated by Smad5 and completely independent of Smad1 before the gastrula stage, whereas at later stages, its expression is dependent upon Smad1 instead of Smad5 (20). These findings suggest that Smad5 acts before gastrulation and is not required during gastrulation in DV patterning. Nevertheless, how other non-Smad5 BMP R-Smads contribute to the patterning of DV axis in zebrafish remains largely unknown. Also, *smad1* and *smad5* are shown to play distinct roles in embryonic hematopoiesis in zebrafish (19).

In this study, we focus on how *smad1*, *smad5*, and *smad9* are differentially regulated and how they cooperatively contribute to early development of zebrafish. We identify a zygotically expressed *smad9* (previously named *smad8*) in the zebrafish genome. The tempo-spatial expression pattern of *smad9* during embryogenesis is similar to that of *smad1*. Although the *smad9* or *smad1* knocked down embryos are not dorsalized, double knockdown of *smad1* and *smad9* leads to strong dorsalization, which cannot be rescued by *smad5* overexpression. By contrast, overexpression of either *smad1* or *smad9* can fully rescue the dorsalized defects in *smad5* morphants. Moreover, the transcriptional onsets of *smad1* and *smad9* are suppressed by each other, and Smad5 binds to the promoter regions and activates the promoter activities of *smad1* and *smad9*. Altogether, our study reveals that *smad1* and *smad9* act redundantly and downstream of *smad5* in regulating zebrafish DV patterning.

## EXPERIMENTAL PROCEDURES

*Animals*—Zebrafish (*Danio rerio*) of the *AB* strain were raised in the China Zebrafish Resource Center (CZRC, Wuhan, China), maintained according to the Zebrafish Book (21), and staged as previously described (22). The experiments involving zebrafish were performed under the approval of the Institutional Animal Care and Use Committee of the Institute of Hydrobiology, Chinese Academy of Sciences.

*Molecular Cloning and Construct Generation*—According to the GenBank™ accession number NM_001004014, full-length zebrafish *smad9* cDNA was amplified from the gastrula cDNA pool by reverse transcription PCR (RT-PCR), using a set of primers, 5′-GGAATTCGAAACAACCCGAATCTCCTG-3′ (P1) and 5′-CCGCTCGAGGTGTCTTGCGTGGCTATG-AAG-3′ (P2). The PCR products were cloned into the EcoRI-XhoI sites of the $pCS2^+$ expression vector and subjected to sequencing. To generate a Smad9-EGFP fusion protein expression construct, *smad9* cDNA was amplified using P1 and 5′-GGG-GTACCTTGGACACCGAGGAAATGGGG-3′ (P3) and cloned into the EcoRI-KpnI sites of the pEGFPN1 vector (Clontech). To generate Smad9-EGFP fusion expression construct that lacks the *smad9* morpholino (MO) binding site, 5′-GGA-ATTCATGCACTCCTCTACCTCCATC-3′ (P4) and P3 were used for PCR amplification, and the PCR products were cloned into the pEGFPN1. To generate a *smad5* expression construct in which the *smad5* MO binding site is mutated, 5′-CGGGAT-CCATGACAAGTATGAGCTCCTTATTTTCCTTCACCA-GCCCG-3′ and T3 primer (5′-ATTAACCCTCACTAA-AGGGA-3′) were used to amplify mutated *smad5* from $pCS2^+$*_zsmad5*, and the PCR products were subcloned into the BamHI-EcoRI sites of $pCS2^+$. The coding sequences of *smad1*, *smad4*, *smad5*, and *smad9* were amplified and subcloned into pHAM, pCMVTag2B, and pCMVTag3C constructs to generate HA-, FLAG-, and Myc-tagged fusion constructs. The putative promoter region of *smad1* was amplified from the zebrafish genomic DNA using the primers 5′-TTTTACCTTC-AGAACTGCCTTAATCCATC-3′ (P5) and 5′-GAGCCATT-CACAAACGTGTCAGTAGTAATCTCA-3′ (P6), and that of *smad9* was amplified with 5′-GCAACTATTAAGAAAACAT-TGCACGGAT-3′ (P7) and 5′-AACTTACTTATGTGGTTG-AAAACGCTCC-3′ (P8). The PCR products were cloned into pGL3-Basic (Promega) to generate constructs for the luciferase assay.

*MO and mRNA Injections*—Antisense MOs (Gene Tools, LLC) were designed to complement the translation start sites of *smad9* (*smad9* MO, 5′-TCGTGAGACGGGTTGATTTTA-AATC-3′) and *smad1* (*smad1* MO, 5′-GGAAAAGAGTGAG-GTGACATTCATT-3′). *smad1* MO has only one base shift compared with the previously published *smad1* MO (19). MO used for knockdown of *smad5* was as described previously (16). To make synthetic capped RNA encoding *smad1*, *smad5*, *smad9*, *bmp2b*, *bmp4*, *bmp7*, and dominant negative BMP receptor 1a (*DNBR1a*), $pCS2^+$-based constructs containing the corresponding cDNA were linearized by NotI, and mRNA was synthesized using the sp6 mMessage mMachine kit (Ambion). For microinjection, embryos were injected with mRNA and morpholinos of interest at the 1-cell stage as described previously (23).

*RNA Isolation, Semiquantitative RT-PCR, and Quantitative RT-PCR*—Total RNA was extracted from embryos and organs with TRIzol reagent following the manufacturer's manual (Invitrogen). 1 $\mu$g of total RNA was used to generate cDNA with first strand Moloney murine leukemia virus reverse transcriptase (Invitrogen) and oligo$(dT)_{20}$ RT primer. The cDNA was then used in a polymerase chain reaction (PCR) accordingly: 95 °C for 5 min; 95 °C for 30 s, 58 °C for 30 s, and 72 °C for 40 s for specific cycles; and 72 °C for 10 min. Primers and amplification cycles for each primer pair used were as follows: *smad1*, 5′-AGAGGTGTATGCCGAATGTTTG-3′ (forward) and 5′-CCATCTGGGTGAGGACTTTATC-3′ (reverse), 26 cycles; *smad5*, 5′-AAAACACCCGTCGCCACATC-3′ (forward) and 5′-AGCCCATCATTACGAGACAGAA-3′ (reverse), 22 cycles; and *smad9*, 5′-GAAGGCTCCAGGTGTCTCAT-3′ (forward) and 5′-GAAGCGGTTCTTGTTGTTTG-3′ (reverse), 26 cycles. An *ef1a*-specific primer pair (forward, 5′-TCACCCTG-

GGAGTGAAACAGC-3′; reverse, 5′-ACTTGCAGGCGATG-TGAGCAG-3′) was used for PCR as an internal control (24). For quantitative PCR, the amplification was performed on a CFX96™ real-time PCR detection system (Bio-Rad) according to the manufacturer's instructions. Primers for *smad5* were 5′-CTTTGAGGCCGTCTATGAGC-3′ (forward) and 5′-GGGT-GCTTGTCACATCTTGT-3′ (reverse). A pair of β-actin primers (forward, 5′-CGAGCAGGAGATGGGAACC-3′; reverse, 5′-CAACGGAAACGCTCATTGC-3′) was used as the internal control (25).

*Luciferase Reporter Assay*—To analyze the putative promoter activities of *smad1* and *smad9* in different genetic background, the relative luciferase activities were determined by the Dual-Luciferase reporter assay system as described previously (26). Each embryo was coinjected with *smad1* promoter-*luc* or *smad9* promoter-*luc* (described previously) and a constitutively expressed *TK-Renilla* luciferase construct (Promega). These embryos were subsequently injected with the indicated RNA or morpholino samples. When the embryos developed to shield stage, sets of 30 embryos were lysed, the luciferase activity was measured with a Promega luminometer, and relative luciferase activity was calculated as described (27). Assays were performed in triplicates, and the average values and the standard variations were calculated. A $p$ value less than 0.05 was considered statistically significant.

*Cycloheximide Treatment*—Embryos were cultured in fish medium containing 50 μg/ml protein synthesis inhibitor cycloheximide (CHX) from 2 h postfertilization (hpf) until the embryos were fixed for whole-mount *in situ* hybridization (28).

*Whole-mount in Situ Hybridization*—Whole-mount *in situ* hybridization (WISH) was performed using digoxigenin (DIG)-labeled antisense RNA probes and anti-DIG alkaline phosphatase-conjugated antibody as described (29). pCS2$^+$ vectors containing *smad1*, *smad5*, and *smad9* were digested with HindIII, and the antisense RNA probes were synthesized with T7 RNA polymerase (Promega). Molecular markers for analyzing DV patterning were *cyp26a* (30), *foxi1* (31), *sizzled* (32), and *ved* (33). Antisense probes of *l-plastin* and *mpx* (34–36) were used to analyze the myelopoiesis in zebrafish development.

*Chromatin Immunoprecipitation*—Chromatin immunoprecipitation (ChIP) assays were performed with a ChIP assay kit (Upstate Biotechnology) as described with some modifications (37). Briefly, 2000 embryos were injected with 300 pg/embryo *HA-smad5* mRNA or *HA-sv40* mRNA. Immunoprecipitation was carried out using anti-HA antibody (Santa Cruz Biotechnology, Inc.). The relative amounts of *smad1* or *smad9* upstream region in immunoprecipitated chromatin and input control were measured using quantitative PCR described previously. The primers specific for the *smad1* upstream region were 5′-AAACATGCACTCTAGCCTTCG-3′ (forward) and 5′-GTAGCCAACTCAATCTGGGAC-3′ (reverse). For the *smad9* promoter region, primers were 5′-GAGTATTGTTAC-GTTCCCCTGCAG-3′ (forward) and 5′-CGCGGATGGATA-CACTTCGA-3′ (reverse). The exon of ribosomal protein *rpl5b* was served as a negative control, and the primers were 5′-GGG-GATGAGTTCAATGTGGAG-3′ (forward) and 5′-CGAACAC-CTTATTGCCAGTAG-3′ (reverse) as described (38).

*Cell Culture, Transfection, Immunoblotting, and Co-immunoprecipitation*—HEK293T cells were grown in Dulbecco's modified Eagle's medium (Invitrogen) plus 10% fetal bovine serum (Hyclone). DNA transfection into HEK293T cells was performed using Vigofect (Vigorous). Immunoprecipitation and immunoblotting were performed as described (39). The FLAG-tagged proteins were immunoprecipitated from cell lysates using agarose-conjugated anti-FLAG antibody (Santa Cruz Biotechnology). Antibodies against HA tag, FLAG tag, and Myc tag were purchased from Sigma-Aldrich and Santa Cruz Biotechnology.

## RESULTS

*smad1 Genetically Interacts with smad5 in Zebrafish DV Patterning*—Previous studies have shown that, although ectopic expression of *smad1* led to strong ventralization of zebrafish (9, 40), knockdown of *smad1* did not give an obvious dorsalization phenotype (19). This is distinct from zebrafish *smad5*, whose gain of function ventralized the embryos and whose loss of function strongly dorsalized the embryos (17, 18). Because both Smad1 and Smad5 are widely believed to be the major transducers of the ventralizing BMP signals, we further asked whether *smad1* carries ventralization activity intrinsically and whether *smad1* genetically interacts with *smad5* in DV patterning. First of all, we injected *in vitro* transcribed enhanced green fluorescent protein (*egfp*) mRNA into 1-cell stage zebrafish embryos. These embryos developed normally and showed normal expression of DV patterning-related genes, so we used uninjected embryos as controls for subsequent analysis. As shown in Fig. 1*B*, when *smad1* mRNA was injected into zebrafish zygotes, the injected embryos were strongly ventralized, as characterized by an expansion of ventral posterior tissues at the expense of dorsal anterior tissues (41). According to the previous study (5), the ventralized embryos at 30 hpf were divided into three classes, V1–V3. Injection of 300 pg of *smad1* mRNA per embryo caused ventralized phenotypes in 74% of the embryos, which were 47% V1 (showing slightly increased ventral tail fin and enlarged blood island), 20% V2 (showing reduced or absent notochord but remained head structures), and 7% V3 (showing absent notochord and anterior structures as well as expanded posterior). These results strongly suggest that zebrafish *smad1* carries ventralization activity.

In order to further analyze the function of *smad1* during DV patterning, translation-blocking MO was utilized for loss-of-function studies. Low dose injection of *smad1* MO (1 ng/embryo) caused no obvious phenotype changes. When the injection dose was raised to 2.4 ng/embryo, the morphants showed degenerated anterior neurons and not well extended yolk stalk as well as slightly extended ventral blood island at 30 hpf (Fig. 1*C*), just like in a previous report (19) demonstrating that *smad1* morphants have an increased number of erythroid cells at the ventral blood island, compared with the wild type embryos (Fig. 1*A*). Therefore, translational block of *smad1* did not cause any dorsalization phenotype in zebrafish embryos, indicating that *smad1* is not required by itself for DV axis establishment.

Then we were interested in the function of *smad1* under conditions in which endogenous Smad5 activity is slightly lessened. We utilized different doses of *smad5* MO to attenuate

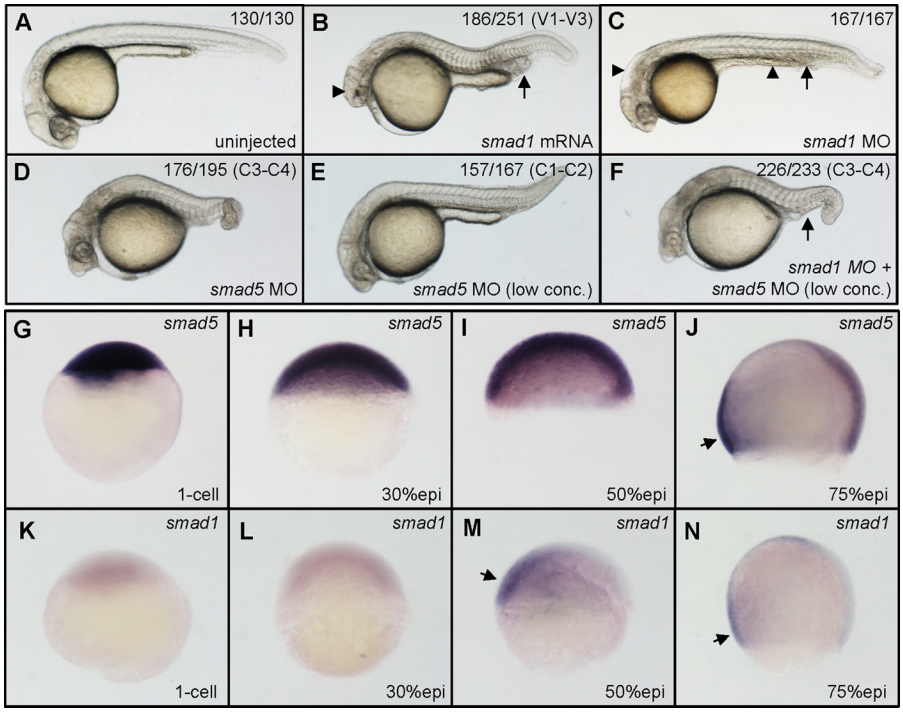


FIGURE 1. ***smad1* genetically interacts with *smad5* in DV patterning.** *A*, an uninjected control embryo. *B*, a typical ventralized embryo that was injected with *smad1* mRNA (300 pg/embryo). *C*, a typical *smad1* morphant that was not dorsalized (2.4 ng/embryo). *D*, a typical dorsalized embryo that was injected with *smad5* MO (1.6 ng/embryo). *E*, a typical weakly dorsalized embryo that was injected with 0.8 ng/embryo *smad5* MO. *F*, a typical *smad1* and *smad5* double morphant (2 ng *smad1* MO + 0.8 ng *smad5* MO per embryo) that was strongly dorsalized. For each injection experiment, over 120 embryos were observed, and a representative phenotype is shown, and the number of embryos showing a corresponding phenotype is indicated in the *top right corner* of each *panel*. *G–J*, WISH analysis of *smad5*. *smad5* is maternally expressed (*G*) and shows ubiquitous expression before gastrulation (*H* and *I*), and its transcripts are more prominently present in the ventral side of the embryo at 75% epiboly stage (*J*). *K–N*, WISH analysis of *smad1*. *smad1* does not show maternal expression (*K*); its zygotic transcription does not begin at 30% epiboly (*L*), and it starts from 50% epiboly (*M*) until the gastrula stage in the ventral side of the embryo (*N*). Embryos in *A–F* are at 30 hpf, shown in a *lateral view* with anterior to the *left*; embryos in *G*, *H*, *K*, and *L* are shown in a *lateral view* with animal pole to the *top*; embryos in *I*, *J*, *M*, and *N* are shown in a *lateral view* with dorsal to the *right*. *Arrow* in *B*, expanded blood island; *arrowhead* in *B*, loss of head structure; *arrowheads* in *C*, thinner yolk and degenerative central neural system; *arrow* in *C*, slightly extended blood island due to increase in erythroid cells; *arrow* in *F*, loss of ventral tissues; *arrows* in *J*, *M*, and *N*, ventral location of signals. *conc.*, concentration; *epi*, epiboly.

Smad5 activity at different levels (16). We observed the dorsalized embryos at 30 hpf with phenotype strength from C1 to C4 (42). Injection of *smad5* MO at a dose of 1.6 ng/embryo produced 36% C4 (showing significant coiling of the tail as well as dorsalization within the anterior regions), 54% C3 (showing shortened and twisted tail), and 10% C2 dorsalization (showing normal tail length with absent ventral tail vein and fin) (Fig. 1*D*). When the injection dose of *smad5* was titrated to 0.8 ng/embryo, however, the injected embryos showed a very mild dorsalization phenotype, with 94% C1-C2 (Fig. 1*E*) and 6% C3. Intriguingly, coinjection of low dose of *smad1* MO (2 ng/embryo) strongly dorsalized the injected embryos, showing 44% C4, 53% C3, and 3% C2 dorsalized embryos (Fig. 1*F*), the phenotype for which was even stronger than with the high dose (1.6 ng/embryo) injection of *smad5* MO alone (36% C4, 54% C3, and 10% C2). Therefore, *smad1* knockdown could strongly amplify the dorsalization effects resulting from mild knockdown of *smad5*, although no DV defects are observed in *smad1* knockdown. Taken together, these findings suggest that *smad5* or its downstream factors could compensate for the activity of *smad1* when *smad1* itself is knocked down.

Because knockdown of *smad1* or *smad5* resulted in distinct phenotypes, we further comparatively analyzed their expression patterns during embryogenesis via WISH. As shown in Fig. 1, *G–J*, *smad5* is maternally expressed, and its transcripts are ubiquitously displayed until midgastrulation, when there is transcriptional enrichment in the ventral side of the embryo. The expression pattern of *smad1* is distinctly different (Fig. 1, *K–N*). *smad1* is not maternally expressed and does not start its transcription until 50% epiboly, before the onset of gastrulation. During gastrulation, its expression is restricted to the ventral side of the embryo.

*smad9 Genetically Interacts with smad5 in Zebrafish DV Patterning*—The aforementioned results suggest that there might be other factors that are downstream of *smad5* to compensate for the activity of Smad1 *in vivo*. This is also supported by the previous study that a maternal-zygotic *smad5* mutant ($sbn^{-/-}$) could be rescued by overexpression of *bmp2b*, indicating that ventral-promoting Smad activity exists in the *smad5* mutants (17). We speculate that another BMP R-Smad, Smad9 (43), might be the factor besides Smad1 that is downstream of Smad5 to induce ventral fate. The full coding region of *smad9* (previously named *smad8*; see the Zebrafish Model Organism Database) was PCR-amplified from a cDNA pool of zebrafish embryos before 24 hpf. The predicted amino acid sequence of Smad9 protein is shown in Fig. 2*A*. Zebrafish Smad9 is closely related to the Smad9 proteins of human, rat, mouse, and *Xenopus*, especially in the MH1 and MH2 domains. All of the three zebrafish BMP R-Smads (Smad1, Smad5, and Smad9) share striking sequence similarities (Fig. 2*B*). The phylogenetic tree of

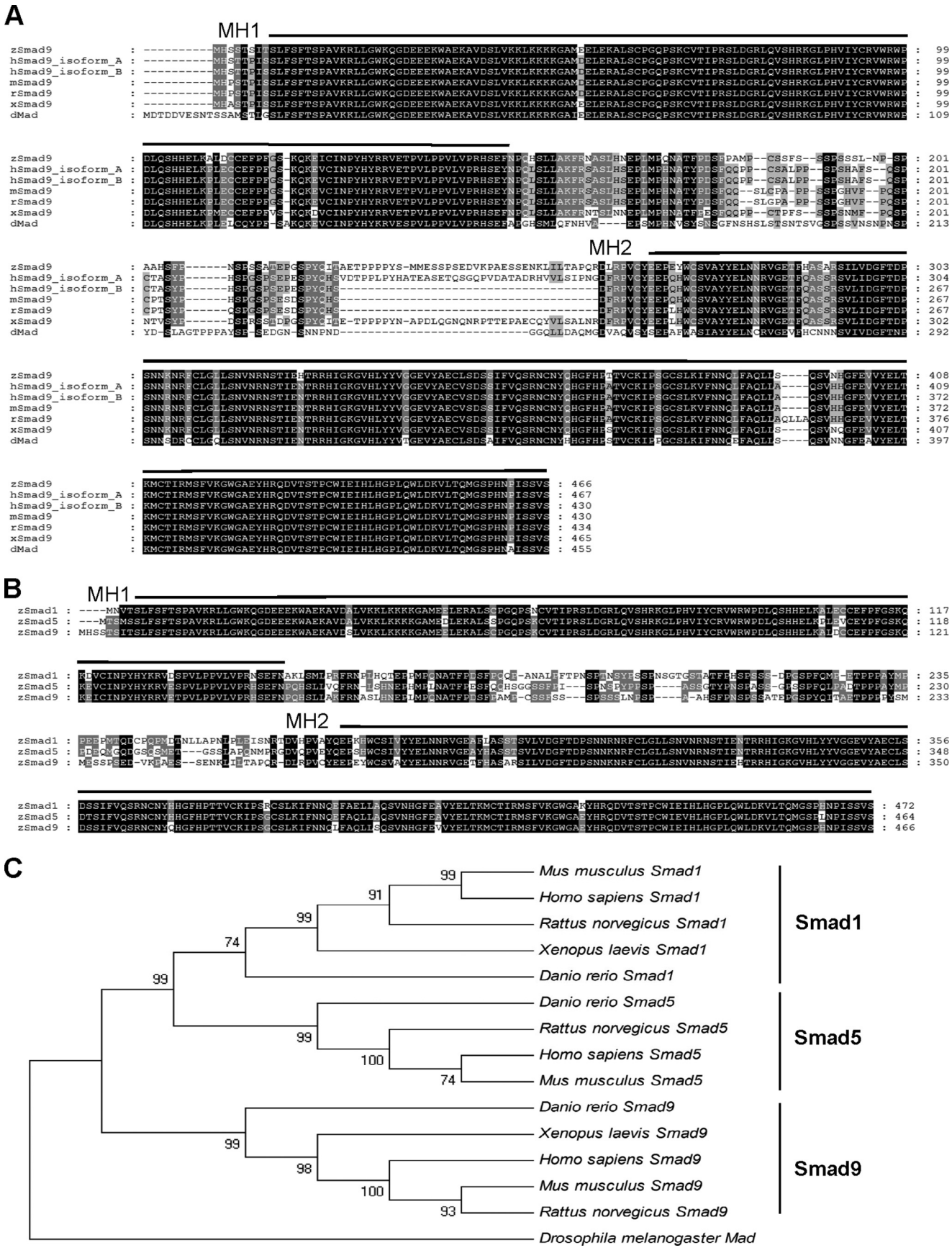
A
MH1
MH2
zSmad9
hSmad9_isoform_A
hSmad9_isoform_B
mSmad9
rSmad9
xSmad9
dMad
B
MH1
MH2
zSmad1
zSmad5
zSmad9
C
Mus musculus Smad1
Homo sapiens Smad1
Rattus norvegicus Smad1
Xenopus laevis Smad1
Danio rerio Smad1
Danio rerio Smad5
Rattus norvegicus Smad5
Homo sapiens Smad5
Mus musculus Smad5
Danio rerio Smad9
Xenopus laevis Smad9
Homo sapiens Smad9
Mus musculus Smad9
Rattus norvegicus Smad9
Drosophila melanogaster Mad
Smad1
Smad5
Smad9

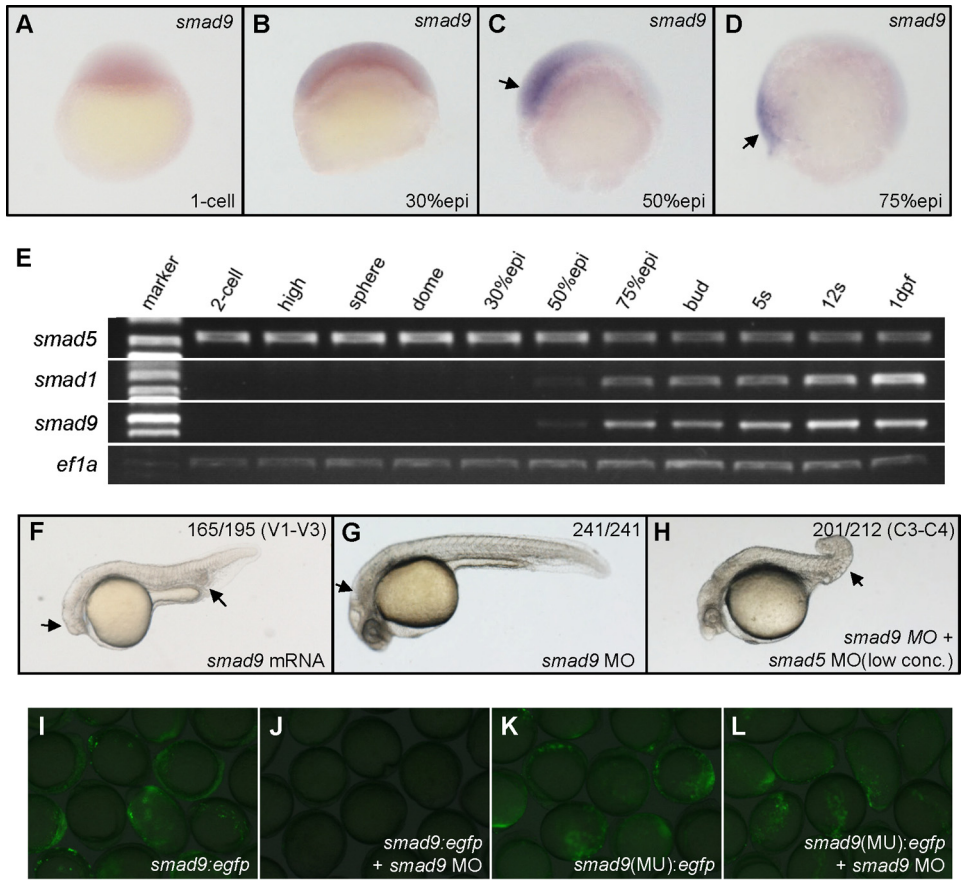


FIGURE 3. ***smad9* genetically interacts with *smad5* in DV patterning.** *A–D*, WISH analysis of *smad9* expression during early development. *smad9* does not show maternal expression (*A*), does not show zygotic expression at 30% epiboly (*B*), and starts its transcription from the 50% epiboly stage in the ventral side of the embryo (*C*) and continues expressing in the ventral side in gastrula stage (*D*). *E*, semiquantitative RT-PCR analysis of *smad1*, *smad5*, and *smad9* during early development. *ef1a* was used as internal control. Only *smad5* has maternal expression, and its transcriptional levels drop from the gastrula stage. *smad1* and *smad9* start to transcribe from the 50% epiboly stage, and their expression levels tend to show an increase during later stages. *F*, a typical ventralized embryo that was injected with *smad9* mRNA (500 pg/embryo). *G*, a typical *smad9* morphant embryo that is not dorsalized (6.4 ng/embryo). *H*, a typical *smad9* and *smad5* double morphant (4 ng of *smad9* MO + 0.8 ng of *smad5* MO per embryo) that is strongly dorsalized. *I–L*, *smad9* morpholino used in the present study is specific and effective. The strong expression of Smad9-EGFP fusion protein (*I*) could be effectively blocked by coinjection of *smad9* MO (*J*). The expression of Smad9(MU)-EGFP fusion protein (*K*) could not be blocked by coinjection of *smad9* MO (*L*). In the *smad9*(MU)-*egfp* construct, the binding site of *smad9* MO is mutated. For each injection experiment, over 120 embryos were observed, and a representative phenotype is shown, and the number of embryos showing corresponding phenotype is indicated in the *top right corner* of each *panel*. Embryos in *A* and *B* are shown in a *lateral view* with animal pole to the *top*; embryos in *C* and *D* are shown in a *lateral view* with dorsal to the *right*; and embryos in *F–H* are at 30 hpf and shown in a *lateral view* with anterior to the *left*. *Arrows* in *C* and *D*, ventrally expressed *smad9* signals; *arrows* in *F*, smaller eyes and enlarged blood island; *arrow* in *G*, degenerative central neural system; *arrow* in *H*, loss of ventral tissues.

R-Smads of several vertebrates shows that the zebrafish Smad9 is clustered with Smad9 rather than Smad1 or Smad5 of other species (Fig. 2*C*). The early expression profile of *smad9* was analyzed by WISH and RT-PCR. As shown in Fig. 3, *A–D*, *smad9* starts its transcription prior to the onset of gastrulation in the ventral side of the embryo and continues its expression in the ventral gastrula, the same as *smad1*. From the results of RT-PCR (Fig. 3*E*), *smad5* has maternal expression, and its expression level decreases during gastrulation. Both *smad1* and *smad9* initiate their transcription from the 50% epiboly stage, and their zygotic expression tends to be stronger throughout development.

The developmental role of zebrafish *smad9* was studied through overexpression and knockdown experiments. First, *smad9* mRNA was synthesized and injected into 1-cell embryos. 68% of those injected embryos were ventralized (Fig. 3*F*), with 46% V1, 18% V2, and 4% V3. This indicates that *smad9* carries intrinsic ventralizing activity, mimicking *smad1*. To knock down Smad9 expression *in vivo*, a translation-blocking MO was employed. To prove the effectiveness and specificity of *smad9* MO (44), we coinjected the MO with the constructs coding for fusion protein Smad9-EGFP with or without the MO binding site separately. In comparison with the strong EGFP signal in the *smad9-egfp* construct-injected embryos (Fig. 3*I*), the MO-coin-

FIGURE 2. **Zebrafish Smad9 is highly homologous with BMP R-Smads among different species.** *A*, the predicted zebrafish Smad9 (*zSmad9*) sequence is aligned with those of human (*h*), mouse (*m*), rat (*r*), *Xenopus* (*x*), and *Drosophila* Mad (*dMad*). Humans have two isoforms of Smad9, indicated as isoform A and isoform B. The MH1 and MH2 domains are highly conserved, whereas the linker regions are more divergent. *B*, comparison of the predicated protein sequences of zebrafish Smad1, Smad5, and Smad9. *C*, a phylogenetic tree of BMP R-Smads of different spices. *MH1*, Mad homologous domain 1; *MH2*, Mad homologous domain 2. Sequence alignments were performed using ClustalW, and phylogenetic alignment was generated using MegAlign.

jected embryos showed depletion of EGFP expression (Fig. 3*J*). In addition, if the MO binding site in *smad9* was mutated, the Smad9(MU)-EGFP expression could not be blocked by coinjection of *smad9* MO (Fig. 3, *K* and *L*). These results provided evidence for the effectiveness and specificity of *smad9* MO. Just like the *smad1* morphants, the *smad9* morphants were not dorsalized, even if the injection dose was as high as 6.4 ng/embryo (Fig. 3*G*). Similarly, *smad9* MO (4 ng/embryo) was coinjected into *smad5* mild morphants (0.8 ng/embryos), and the double morphants were analyzed for DV patterning defects at 30 hpf. As shown in Fig. 3*H*, the double morphant embryos were strongly dorsalized, with C4 of 40%, C3 of 55%, and C2 of 5%. The results show that *smad9* knockdown could strongly strengthen the dorsalization of *smad5* mild morphants. Therefore, we conclude that *smad9* genetically interacts with *smad5* in DV pattering of zebrafish *in vivo*.

*Double Knockdown of smad1 and smad9 Leads to Strong Dorsalization*—Altogether, the expression patterns of *smad1* and *smad9* are fairly similar to each other, and so are their overexpression and knockdown effects. The above results reveal that, although *smad1* or *smad9* is not essential by itself for the early DV axis establishment, they could help to pattern the DV axis in a condition in which Smad5 activity is slightly lessened. We further asked whether and how *smad1* and *smad9* cooperatively act in zebrafish DV patterning. A reasonable hypothesis is that *smad1* and *smad9* may function redundantly to each other; *i.e.* if only one of the redundant partners is inhibited, the other partner can be stimulated and compensate for the loss-of-function effects, and the overall amount of partners will not be affected (45). Therefore, in our case, the DV patterning might not be disrupted if *smad1* or *smad9* is knocked down alone. To examine this hypothesis, *smad1* MO (2 ng/embryo) and *smad9* MO (4 ng/embryo) were coinjected into embryos to knock down *smad1* and *smad9* simultaneously. The double morphants were allowed to develop to 30 hpf for analysis of DV defects. Intriguingly, double knockdown of *smad1* and *smad9* strongly dorsalized the embryos with 100% penetration (Fig. 4*C*), showing 69% C4, 28% C3, and 3% C2. This phenotype has never been observed in the single knockdown experiment of *smad1* or *smad9*, which strongly supports the hypothesis that *smad1* and *smad9* have functional redundancy in regulating zebrafish DV patterning.

To further confirm the DV defects in different morphants, the expression of a set of molecular markers indicating DV patterning was analyzed. At the gastrula stage, *cyp26a* labels neuroectoderm territory (30), *foxi1* labels epidermal ectoderm (31), and *sizzled* (*szl*) represents a BMP signaling target (32). As shown in Fig. 4*G*, the expression patterns of these markers were not changed in the *smad1* morphants (*b*, *i*, and *p*) or in the *smad9* morphants (*c*, *j*, and *q*) (the WISH embryos shown in the Fig. 5*G* represent over 90% of the embryos assayed). In *smad1* and *smad9* double morphants, however, the expression of *cyp26a* was remarkably expanded toward the ventral side of the ectoderm (Fig. 4*G*, *f*), whereas the expression of *foxi1* and *szl* was significantly reduced (Fig. 4*G*, *m* and *t*). These results were in accordance with the phenotypic analysis. Similar results of another target gene of BMP signaling, *ved*, were also obtained (data not shown). Therefore, we conclude that *smad1* and *smad9* act redundantly to each other in regulating DV patterning of zebrafish embryos.

Because the phenotype of *smad1* and *smad9* double morphants is similar to that of *smad5* morphants, and it is suggested that *smad1* might be a transcriptional target of *smad5* (9), the relationship among all of these Smads was extensively analyzed. First, we asked whether the dorsalized phenotype of *smad5* morphants could be rescued by overexpression of *smad1* or *smad9*. As shown in Fig. 4, the dorsalization caused by injection of *smad5* MO (36% C4, 54% C3, and 10% C2; Fig. 4*B*) could be rescued by coinjection of *smad1* mRNA (22% C3, 28% C2, and 50% wild type-like; Fig. 4*D*) or *smad9* mRNA (22% C3, 32% C2, and 46% wild type-like; Fig. 4*E*). Second, we asked whether the dorsalization phenotype resulting from *smad1* and *smad9* double knockdown could be rescued by *smad5* overexpression. Surprisingly, the strong dorsalization of *smad1* and *smad9* double morphants (69% of C4, 28% of C3, and 3% of C2) could not be effectively rescued by *smad5* mRNA injection at different doses (67% C4, 26% C3, and 7% C2; Fig. 4*F*). The phenotypic results were further confirmed by WISH analysis with a set of molecular markers representing DV patterning and BMP signaling activity. As shown in Fig. 4*G*, *smad5* morphants showed typical dorsalization of the ectoderm, with enlarged *cyp26a*-labeled and decreased *foxi1*-labeled territories (Fig. 4*G*, *d* and *k*) and a strong reduction of BMP signaling activity (Fig. 4*G*, *r*). Whereas in the *smad5* MO- and *smad1* or *smad9* mRNA-coinjected embryos, the neuroectoderm territories were restored to the normal region or even reduced (Fig. 4*G*, *e*), the non-neural ectoderm expressing *foxi1* labeled a much wider region (Fig. 4*G*, *l*), and *szl* expression was restored to the normal level (Fig. 4*G*, *s*). By contrast, the dorsalized phenotype of *smad1* and *smad9* double morphants could not be efficiently rescued by overexpression of *smad5* (Fig. 4*G*, *g*, *n*, and *u*). The inability of ectopic *smad5* overexpression to efficiently rescue the DV patterning defects in *smad1* and *smad9* double morphants suggests that Smad5 has transcriptional and functional activities differing from Smad1 and Smad9.

*smad1 and smad9 Are Downstream Targets of smad5*—To further clarify the regulation network among *smad1*, *smad5*, and *smad9*, we analyzed the transcription of different BMP type *smad* genes in *smad1*, *smad5*, or *smad9* knocked down or overexpressed embryos at 50% epiboly, a stage when *smad1* and *smad9* start their zygotic transcription. Just as reported previously (9), *smad1* transcription was strongly induced by *smad5* misexpression (Fig. 5*A*, *b*), and *smad1* transcription was absent if *smad5* was knocked down (Fig. 5*A*, *c*). Similarly, the transcription of *smad9* strongly increased in the *smad5* overexpressed embryos (Fig. 5*A*, *l*) and nearly disappeared in *smad5* morphants (Fig. 5*A*, *m*).

To better understand the transcriptional regulation of these *smad* genes, we further cloned the upstream regulatory region of *smad1* of 4290 bp and the upstream regulatory sequence of *smad9* of 3456 bp and utilized them to generate two luciferase assay constructs. Relative luciferase assays revealed that the activity of the *smad1* promoter was significantly elevated to 2.72-fold by overexpression of *smad5* and significantly decreased to 0.50-fold by knockdown of *smad5* in the embryos at the 50% epiboly stage (Fig. 5*B*). Likewise, *smad9* promoter activity showed a significant

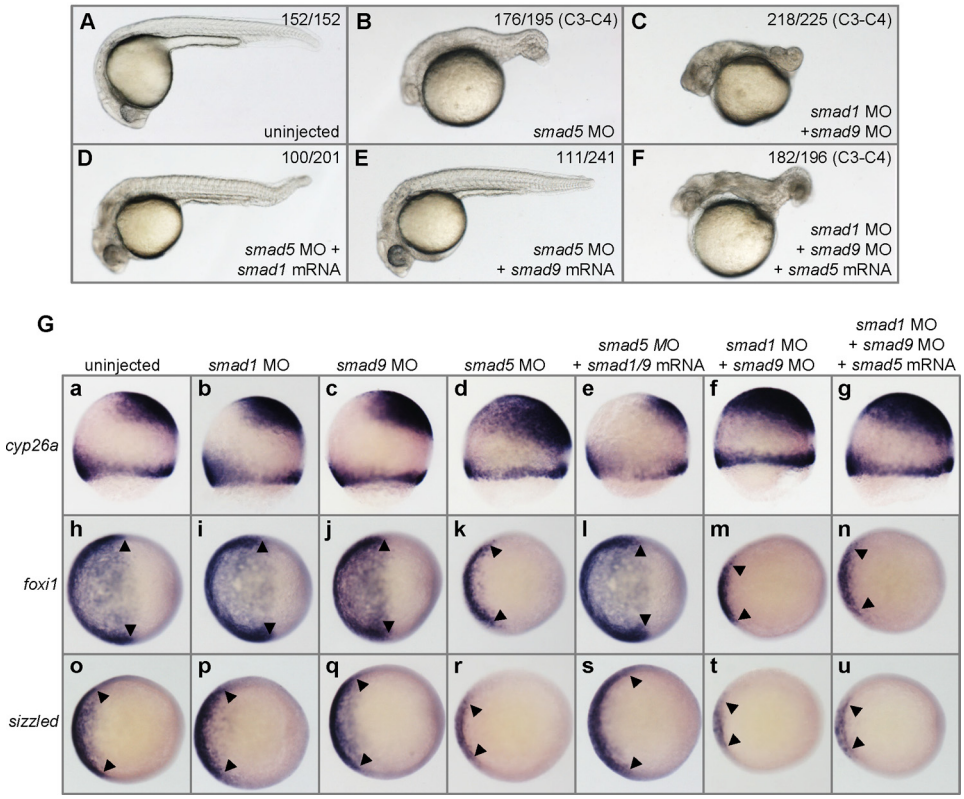


FIGURE 4. **Double knockdown of *smad1* and *smad9* leads to strong dorsalization that cannot be rescued by *smad5* overexpression.** *A*, a typical uninjected control embryo. *B*, a typical *smad5* morphant (1.6 ng/embryo) showing a strong dorsalized phenotype. *C*, a typical *smad1* and *smad9* double morphant (2 ng of *smad1* MO + 4 ng of *smad9* MO per embryo) that is strongly dorsalized. *D*, a typical rescued embryo resulting from coinjection of *smad5* MO (1.6 ng/embryo) and *smad1* mRNA (200 pg/embryo). *E*, a typical rescued embryo resulting from coinjection of *smad5* MO (1.6 ng/embryo) and *smad9* mRNA (300 pg/embryo). *F*, a typical dorsalized embryo that was coinjected with *smad1* MO (2 ng/embryo) and *smad9* MO (4 ng/embryo) and *smad5* mRNA (300 ng/embryo). For each injection experiment, over 120 embryos were observed, and a representative phenotype is shown, and the number of embryos showing corresponding phenotype is indicated in the *top right corner* of each *panel*. *G*, WISH analysis of the embryos injected with different reagents. Embryos were uninjected control or injected with MOs and mRNAs indicated at the *top* of each *column*. *a–g*, *cyp26a* staining, which labels neuroectoderm; *h–n*, *foxi1* staining, which labels epidermal ectoderm; *o–u*, RNA *in situ* labeling by *szl*, which is a BMP target. *b*, *i*, *p*, *c*, *j*, and *q*, in *smad1* MO- or *smad9* MO-injected embryos, the expression of DV patterning markers was the same as that in the control embryos (*a*, *h*, and *o*). *d*, *k*, and *r*, in *smad5* MO-injected embryos, the expression level of the *cyp26a* is elevated, and the expression of *foxi1* and *szl* is strongly reduced. *e*, *l*, and *s*, in *smad5* morphants coinjected with *smad1* or *smad9* mRNA, the enlarged expression of *cyp26a* is rescued to normal and the reduced expression of *foxi1* and *szl* is also rescued to wild type level; *f*, *m*, and *t*, in *smad1* and *smad9* double morphants, the expression of *cyp26a* is strongly increased, and the expression of *foxi1* and *szl* is strongly reduced. *g*, *n*, and *u*, the alteration of the expression of these markers in *smad1* and *smad9* double morphants cannot be rescued by *smad5* mRNA injection. Embryos in *A–F* are shown in a *lateral view* with anterior to the *left*, 30 hpf; embryos in *G*, *row 1*, are at the 70% epiboly stage, shown in a *lateral view* with dorsal to the *right*; embryos in *G*, *row 2*, are at 70% epiboly, shown in an *animal pole view* with dorsal to the *right*; and embryos in *G*, *row 3*, are at the 60% epiboly stage, shown in an *animal pole view* with dorsal to the *right*. The results shown in *G* for WISH analysis represent over 90% of the embryos assayed.

increase to 1.99-fold by *smad5* overexpression and a significant decrease of 0.56-fold by *smad5* knockdown (Fig. 5*C*). These findings reveal that the transcription of both *smad1* and *smad9* is dependent on *smad5* and is positively regulated by *smad5*.

To clearly elucidate the transcriptional regulation between *smad1* and *smad9*, we conducted transcriptional analysis of *smad1* or *smad9* in the embryos with up- or down-regulation of *smad1* or *smad9*. First, *smad9* mRNA or *smad9* MO was injected into zebrafish embryos, and the injected embryos at 50% epiboly were subjected to WISH analysis of *smad1*. Strikingly, the transcription initiation of *smad1* was highly repressed by *smad9* overexpression (Fig. 5*A*, *e*) and significantly enhanced by *smad9* knockdown (Fig. 5*A*, *f*). Second, *smad1* mRNA or *smad1* MO was injected, and the embryos at 50% epiboly were subjected to WISH analysis of *smad9*. The labeling signals of *smad9* nearly disappeared in the *smad1*-overexpressed embryos (Fig. 5*A*, *n*), and the signals dramatically increased in the *smad1* knocked down embryos (Fig. 5*A*, *o*). This demonstrates that the transcriptional onset of *smad1* and of *smad9* are negatively regulated by each other. Third, this conclusion was further confirmed by promoter activity analysis by luciferase assays. As expected, in *smad9*-overexpressed embryos, the activity of the *smad1* promoter was down-regulated to 0.58-fold, and in *smad9* morphants, it was up-regulated to 1.63-fold (Fig. 5*B*). Similarly, the activity of *smad9* promoter was down-regulated to 0.56-fold in *smad1*-overexpressed embryos and up-regulated to 1.49-fold in *smad1* morphants (Fig. 5*C*). Taken together, these results reinforce the notion that *smad1* and *smad9* act redundantly to each other at the transcriptional level, and these also give a reasonable explanation why double knockdown instead of single knockdown of *smad1* or *smad9* induces visible dorsalization effects.

In addition, we analyzed the regulation effects of *smad1* and *smad9* on themselves and on *smad5*. In *smad1* knocked down embryos, the transcription of *smad1* was strongly elevated (Fig. 5*A*, *d*), suggesting that *smad1* is negatively self-regulated. In

*smad1* MO- and *smad9* MO-coinjected embryos, the expression level of *smad1* was dramatically elevated (Fig. 5*A*, *g*), higher than that in *smad1* MO- or *smad9* MO-injected embryos at the 50% epiboly stage, whereas coinjection of neither *smad1* MO nor *smad9* MO with *smad5* MO could restore the transcription of *smad1* (Fig. 5*A*, *h* and *i*), confirming that *smad1* is downstream of *smad5*. In *smad1* MO-, *smad9* MO-, and *smad5* mRNA-coinjected embryos, the expression of *smad1* was greatly enhanced, spreading to the whole blastomere (Fig. 5*A*, *j*). Likewise, *smad9* was negatively self-regulated; as in *smad9* MO-injected embryos, the labeling signals of *smad9* by WISH were strongly elevated (Fig. 5*A*, *p*). Additionally, the signals of

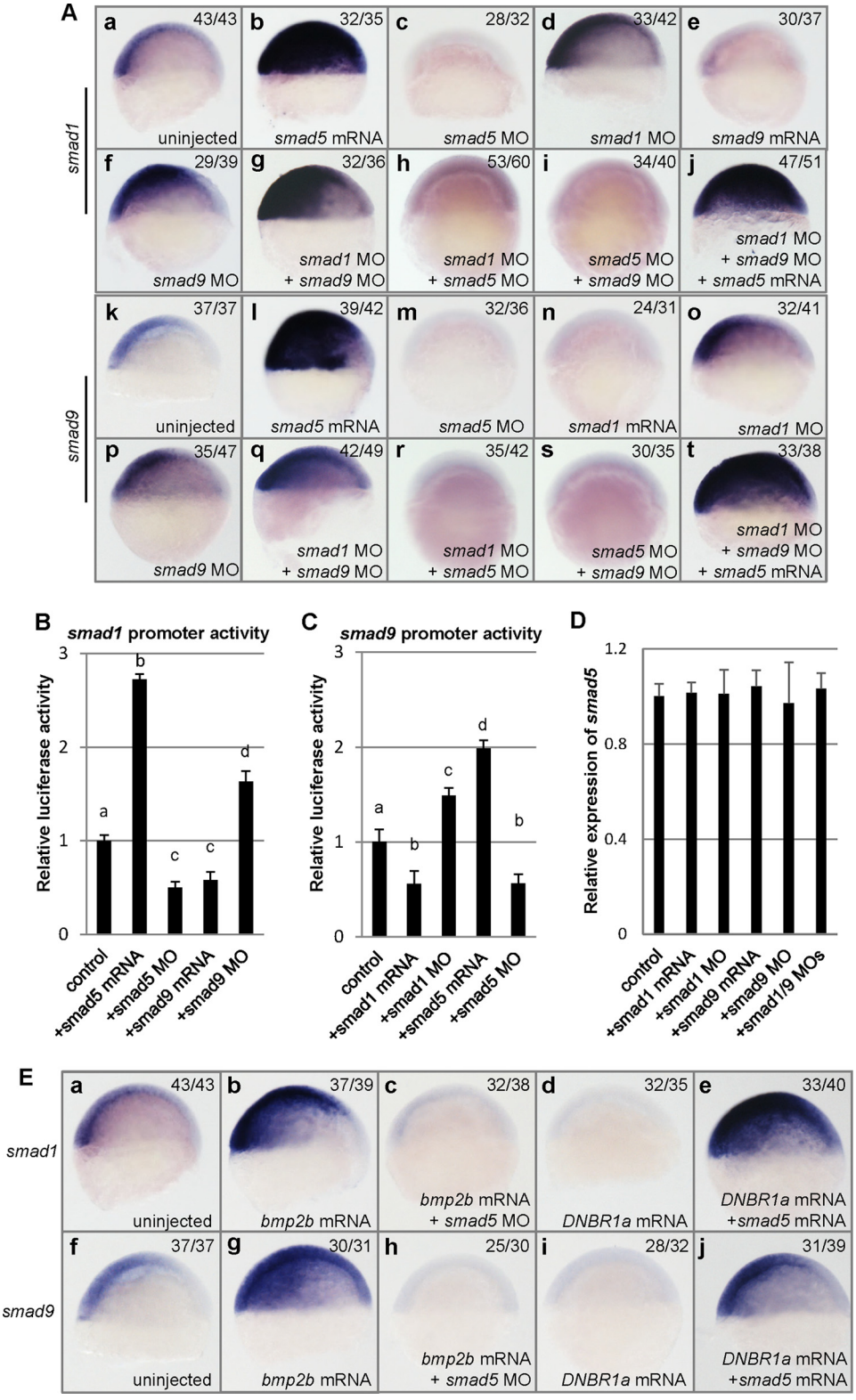

*smad9* increased even more in *smad1* and *smad9* double morphants (Fig. 5*A*, *q*), whereas in the background of *smad5* morphants, neither knockdown of *smad1* nor knockdown of *smad9* could rescue the disappearance of *smad9* transcription (Fig. 5*A*, *r* and *s*), confirming that *smad9* is downstream of *smad5*. The strongest signal of *smad9* was observed in *smad1* MO-, *smad9* MO-, and *smad5* mRNA-coinjected embryos (Fig. 5*A*, *t*). On the other hand, the potential transcriptional regulation of *smad5* by *smad1* and *smad9* was analyzed by quantitative RT-PCR (Fig. 5*D*). The amount of *smad5* transcripts in *smad1* mRNA-, *smad1* MO-, *smad9* mRNA-, or *smad9* MO-injected embryos showed no significant difference when compared with wild type at 50% epiboly as well as with the embryos coinjected with *smad1* MO and *smad9* MO. These results further demonstrate that both *smad1* and *smad9* locate downstream of *smad5*, and neither of them exert any effects on the transcriptional regulation of *smad5.*

To analyze the transcriptional regulation of *smad1* and *smad9* by *smad5* under different BMP signaling backgrounds, BMP activity-elevated and -abolished embryos were used for further study. As expected, elevated *smad1* transcription was observed in *bmp2b*-overexpressed embryos (Fig. 5*E*, *b*) (9). In order to deplete the overall BMP signaling, a truncated dominant negative BMP receptor 1a, *DNBR1a* (46), was overexpressed in the embryos. In the *DNBR1a* mRNA-injected embryos, the transcription of *smad1* was completely abolished (Fig. 5*E*, *c*), further showing that *smad1* itself is a transcriptional target of BMP signaling. In *bmp2b*-overexpressed embryos, an enlarged domain and higher level of the *smad9* expression were also observed (Fig. 5*E*, *g*), and in *DNBR1a* mRNA-injected embryos, *smad9* transcription was likewise completely inhibited (Fig. 5*E*, *h*). Therefore, the normal transcription of *smad9* also relies on proper BMP signaling activity. However, even in the *bmp2b*-overexpressed embryos, knockdown of *smad5* could still efficiently block the transcription of *smad1* or *smad9* (Fig. 5*E*, *c* and *h*), suggesting that *smad5* is necessary to mediate BMP-induced *smad1* and *smad9* transcription. By contrast, *smad5* overexpression still strongly activated the transcription of *smad1* and *smad9* in the BMP-abolished embryos (Fig. 5*E*, *e* and *j*). These suggest that *smad1* and *smad9* are the direct transcriptional targets of *smad5*, and their transcriptional activities directly rely on *smad5*.

*smad1 and smad9 Are Direct Transcriptional Targets of smad5*—In order to uncover whether there is a direct or indirect effect of *smad5* on activating *smad1* and *smad9*, we used the translation inhibitor CHX from 2 hpf onward to block translation of the earliest zygotic mRNAs but allow the translation of injected *smad5* mRNA (47). Transcriptional induction of *ntl* (no tail) requires intermediate zygotic translation steps after midblastula transition (MBT); thus, the absence of *ntl* signal served as a control of efficiency of CHX treatment (38) (Fig. 6*A*, *a* and *b*). We injected *smad5* MO into 1-cell stage embryos to block the translation of maternal supplied *smad5* transcripts, and as a result, the transcription of *smad1* and *smad9* was absent in the *smad5* MO-injected embryos (Fig. 6*A*, *d* and *h*). After coinjection of mutated *smad5* mRNA whose *smad5* MO binding site was mutated but coding protein was not altered, the signals of *smad1* or *smad9* were restored and elevated in *smad5* morphants (Fig. 6*A*, *e* and *i*). When CHX was added at 2 hpf, expression of *smad1* and *smad9* could still be rescued (Fig. 6*A*, *f* and *j*), indicating that *smad1* and *smad9* are the direct targets of Smad5. To further prove this, we performed a ChIP assay with extracts from embryos at the 50% epiboly stage injected with mRNA encoding HA-tagged Smad5. The precipitated chromatin was then analyzed by quantitative PCR using primer pairs that could amplify segments of the *smad1* promoter or *smad9* promoter. A segment of the *rpl5b* exon amplified by a specific primer pair was used as control (38). As shown in Fig. 6*B*, we observed a significant enrichment for the promoter regions of *smad1* and *smad9* in the immunoprecipitate from the injected samples compared with the *HA-sv40* mRNA-injected control. In contrast, there was no enrichment of the control genomic region *rpl5b*. Thus, these data demonstrate that Smad5 directly binds to the promoters of *smad1* and *smad9* to activate their transcription.

In order to address the intrinsic differences of Smad5, Smad1, and Smad9 proteins, we conducted co-immunoprecipitation experiments to analyze and compare their binding ability

FIGURE 5. ***smad1* and *smad9* are positively regulated by *smad5* and suppress each other.** *A*, WISH analysis of *smad1* (*a–j*) and *smad9* (*k–t*) in different types of embryos injected with different reagents. Compared with wild type embryos (*a*), the transcription of *smad1* is up-regulated by injection of *smad5* mRNA (*b*), *smad1* MO (*d*), or *smad9* MO (*f*) and by coinjection of *smad1* MO and *smad9* MO (*g*) or by coinjection of *smad1* MO, *smad9* MO, and *smad5* mRNA (*j*); the transcription of *smad1* is down-regulated by injection of *smad5* MO (*c*) or *smad9* mRNA (*e*) and by coinjection of *smad1* MO and *smad5* MO (*h*) or by coinjection of *smad5* and *smad9* MO (*i*). Compared with wild type embryos (*k*), the transcription of *smad9* is up-regulated by injection of *smad5* mRNA (*l*), *smad1* MO (*o*), or *smad9* MO (*p*) and by coinjection of *smad1* MO and *smad9* MO (*q*) or by coinjection of *smad1* MO, *smad9* MO, and *smad5* mRNA (*t*); the transcription of *smad9* is down-regulated by injection of *smad5* MO (*m*) or *smad1* mRNA (*n*) and by coinjection of *smad1* MO and *smad5* MO (*r*) or by coinjection of *smad5* MO and *smad9* MO (*s*). *B*, luciferase assay of zebrafish *smad1* promoter activity. The activity of the *smad1* promoter was up-regulated to 2.72-fold by *smad5* mRNA injection and down-regulated to 0.58-fold by *smad9* mRNA injection, and it was down-regulated to 0.50-fold by *smad5* MO injection and up-regulated to 1.63-fold by *smad9* MO injection. *C*, luciferase assay of zebrafish *smad9* promoter activity. The activity of the *smad9* promoter was up-regulated to 1.99-fold by *smad5* mRNA injection and down-regulated to 0.55-fold by *smad1* mRNA injection, and it was down-regulated to 0.56-fold by *smad5* MO injection and up-regulated to 1.49-fold by *smad1* MO injection. In *B* and *C*, embryo lysates were prepared at 5.4 hpf, and the luciferase activities were normalized to *Renilla* luciferase from pRL-TK; results were expressed relative to luciferase activities with constructs alone; each *bar* presents the mean value and the corresponding S.D. (*error bar*) from triplicate analysis. A statistically significant difference ($p < 0.05$) is indicated by a different *lowercase letter above* the *bar*. *D*, relative expression of *smad5* in 50% epiboly embryos injected with different reagents by quantitative PCR analysis. All of the injected samples have no significant difference compared with uninjected control ($p > 0.1$). *E*, WISH analysis of *smad1* (*a–e*) and *smad9* (*f–j*) in the embryos injected with different reagents. *a*, a typical control embryo showing normal expression of *smad1*. *b*, a typical embryo that was injected with *bmp2b* mRNA (20 pg/embryo) with elevated expression of *smad1*. *c*, a typical embryo that was injected with *bmp2b* mRNA (20 pg/embryo) and *smad5* MO (1.6 ng/embryo), showing absent expression of *smad1*. *d*, a typical embryo that was injected with *DNBR1a* mRNA (100 pg/embryo), showing absent expression of *smad1*. *e*, a typical embryo that was injected with *DNBR1a* mRNA (100 pg/embryo) and *smad5* mRNA (300 ng/embryo), showing strong expression of *smad1*. *f*, a typical control embryo showing normal expression of *smad9*. *g*, a typical embryo that was injected with *bmp2b* mRNA (20 pg/embryo), with elevated expression of *smad9*. *h*, a typical embryo that was injected with *bmp2b* mRNA (20 pg/embryo) and *smad5* MO (1.6 ng/embryo), showing absent expression of *smad9*. *i*, a typical embryo that was injected with *DNBR1a* mRNA (100 pg/embryo), showing absent expression of *smad9*. *j*, a typical embryo that was injected with *DNBR1a* mRNA (100 pg/embryo) and *smad5* mRNA (300 ng/embryo), showing strong expression of *smad9*. All embryos in *E* are at the 50% epiboly stage, shown in a *lateral view* with dorsal to the *right*.

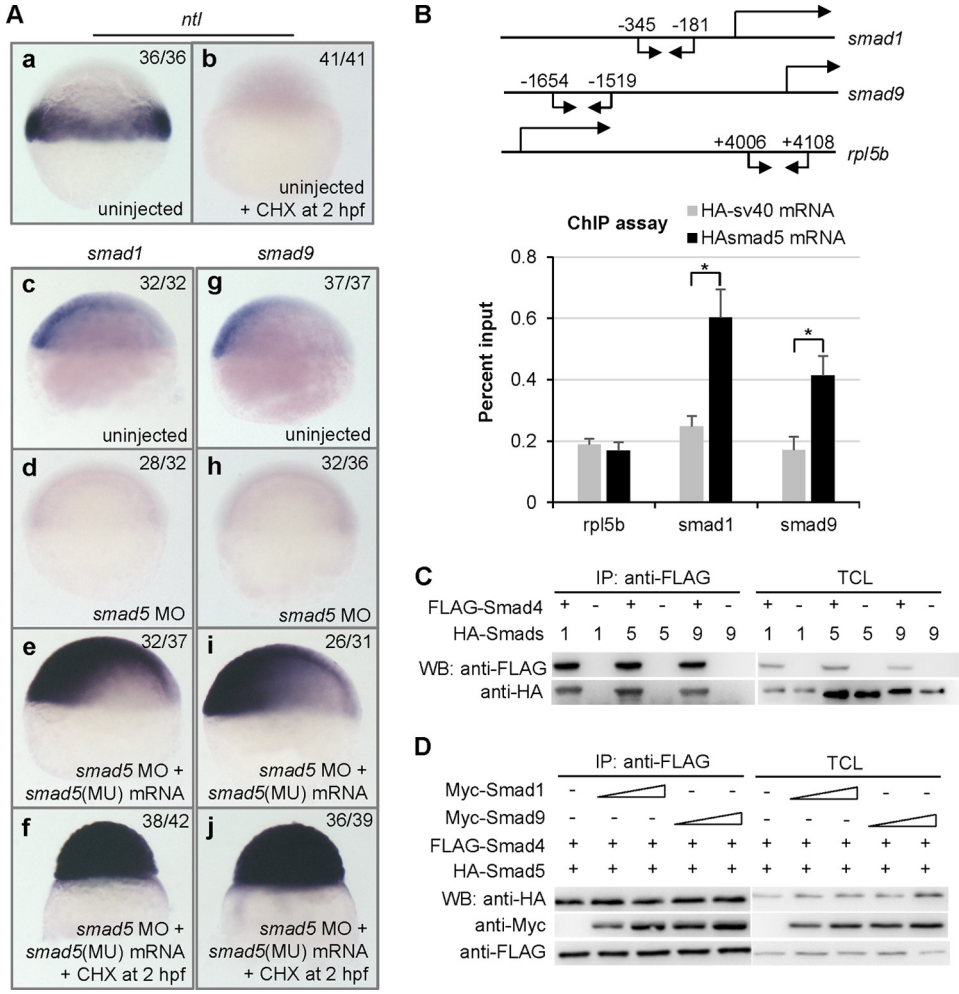


FIGURE 6. ***smad1* and *smad9* are direct transcriptional targets of Smad5.** *A*, WISH analysis of 6 hpf embryos injected with different reagents and treated by CHX or not. *a*, a typical control embryo showing normal expression of *ntl*. *b*, a typical embryo treated by CHX from 2 hpf, showing absent expression of *ntl*. *d* and *h*, embryos injected with *smad5* MO, showing absent expression of *smad1* (*d*) and *smad9* (*h*). *e* and *i*, embryos coinjected with *smad5* MO and mutated *smad5* mRNA, showing restored and elevated expression of *smad1* (*e*) and *smad9* (*i*). *f* and *j*, embryos coinjected with *smad5* MO and mutated *smad5* mRNA and treated by CHX from 2 hpf, showing elevated expression of *smad1* (*f*) or *smad9* (*j*). In *smad5* (*MU*) mRNA, the *smad5* MO binding site is mutated, but the protein sequence coded by the mutated mRNA is identical to that coded by the wild type mRNA. All embryos shown in *A* are in a *lateral view* with animal pole to the *top* or dorsal to the *right*. *B*, ChIP analysis of *HA-smad5* mRNA- or *HA-sv40* mRNA-injected embryos with anti-HA antibody. A *schematic diagram* depicts the fragments of the *smad1*, *smad9*, and *rpl5b* genes that were amplified. The positions of quantitative PCR primers that were used to amplify *smad1* and *smad9* promoter fragments and the *rpl5b* exon fragment are indicated by *arrows*. Chromatin from *HA-smad5* mRNA-injected (*black bars*) and *HA-sv40* mRNA-injected (*gray bars*) embryos was sonicated and immunoprecipitated with anti-HA antibody. DNA levels of *smad1* and *smad9* promoter region and control sequence (*rpl5b* exon) in precipitate and input were measured by quantitative PCR. The *smad1* promoter region was 2.43-fold enriched, and the *smad9* promoter region was 2.44-fold enriched in the *HA-smad5* mRNA-injected samples in comparison with the *HA-sv40* mRNA-injected samples, whereas *rpl5b* did not show enrichment. Each *bar* presents the mean value and the corresponding S.D. (*error bar*) from triplicate analysis. *, statistically significant difference ($p < 0.05$). *C*, Smad4 interacts with Smad1, Smad5, and Smad9. HEK293T cells were transfected with *FLAG-smad4* and *HA-smad1*, *HA-smad5*, or *HA smad9*. FLAG-Smad4-binding proteins were immunoprecipitated and analyzed by immunoblotting. *D*, binding affinity of FLAG-Smad4 against HA-Smad5 is not affected by coexpression of an increasing amount of Myc-Smad1 (1.2 and 2.5 $\mu$g) or Myc-Smad9 (1.2 and 2.5 $\mu$g). *IP*, immunoprecipitation; *TCL*, total cell lysate; *WB*, Western blot.

to Smad4, which is the co-Smad of BMP signaling (48, 49). We first investigated the interaction between zebrafish Smad4 and Smad1/Smad5/Smad9. In HEK293T cells, all of the zebrafish Smad1, Smad5, and Smad9 could bind to Smad4 (Fig. 6*C*). Then we analyzed whether the presence of Smad1 and Smad9 could disturb the binding affinity between Smad5 and Smad4. As shown in Fig. 6*D*, when Smad1 and Smad9 were transfected at increasing doses, the interaction of Smad4 and Smad5 was not affected.

*smad9, Like smad1, Is Required for Myelopoiesis*—It has been reported that *smad1* and *smad5* differently regulate zebrafish embryonic hematopoiesis; *smad1* but not *smad5* is required for the differentiation of macrophages and granulocytes, both belonging to the myeloid lineage (19). Because *smad9* and *smad1* have shown similar expression patterns and regulatory network in zebrafish early development, we proposed that they may share similar functions during embryonic hematopoiesis. First, *smad9* was knocked down or overexpressed in zebrafish embryos, and the injected embryos at 24 hpf were subjected to analysis with a set of myelopoiesis-related markers. As shown in Fig. 7 (*D* and *L*), macrophages labeled by *l-plastin* and granulocytes labeled by *mpx* were obviously diminished in *smad9* morphants at 24 hpf, which just mimicked the *smad1* morphants (Fig. 7, *C* and *K*). This was distinctly different from what was observed in *smad5* morphants, which did not show obvious defects of *l-plastin*- and *mpx*-labeled cells (Fig. 7, *B* and *J*).

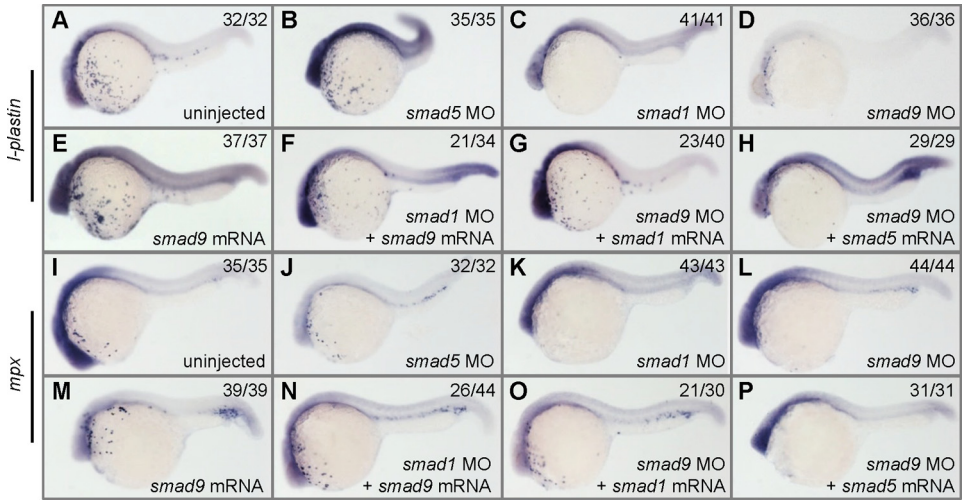


FIGURE 7. ***smad1* and *smad9* regulate the differentiation of macrophages and granulocytes.** Embryos were either uninjected control or injected with different mRNAs and MOs indicated in the images and processed at 24 hpf for WISH to identify *l-plastin* (*A–H*) and *mpx* (*I–P*) transcripts. *l-plastin* labels macrophages, and *mpx* labels granulocytes. The expression of *l-plastin* and *mpx* is normal in *smad5* morphants (*B* and *J*) but is almost completely depleted in *smad1* morphants (*C* and *K*), greatly reduced in *smad9* morphants (*D* and *L*), and slightly increased in *smad9* mRNA-injected embryos (*E* and *M*). Overexpression of *smad1* or *smad9* can rescue the absence of *l-plastin*- and *mpx*-labeled cells in the morphants of each other (*F*, *G*, *N*, and *O*). In contrast, overexpression of *smad5* is unable to rescue the loss of these two types of cells in *smad1* or *smad9* morphants (*H* and *P*). For each assay, over 29 embryos were observed, and a representative phenotype is shown, and the number of embryos showing the corresponding phenotype is indicated in the *top right corner* of each *panel*. The injection doses of the mRNAs are as follows: *smad1* mRNA, 150 pg/embryo; *smad5* mRNA, 200 pg/embryo; *smad9* mRNA, 250 pg/embryo. All embryos are shown in a *lateral view* with anterior to the *left*.

This revealed that *smad9*, like *smad1*, is required for zebrafish myelopoiesis. Second, *smad9* mRNA was injected into *smad1* morphants to check whether *smad9* is able to replace the function of *smad1* in myelopoiesis and vice versa. Coinjection of *smad9* mRNA was able to rescue the developmental defects of *l-plastin*-labeled macrophages in *smad1* morphants in 61% of the embryos (Fig. 7*F*) and *mpx*-labeled granulocytes in 59% of the embryos (Fig. 7*N*), and coinjection of *smad1* mRNA could also restore the myeloid development in the *smad9* morphants (Fig. 7, *G* and *O*; 57% rescue for macrophages and 70% rescue for granulocytes). In contrast, coinjection of *smad5* mRNA was not able to rescue the defects of macrophages and granulocytes in *smad9* morphants (Fig. 7, *H* and *P*; 100%), just like in the previous report (19) in which *smad5* overexpression did not rescue the myeloid defects in *smad1* morphants. Therefore, our study reveals that *smad1* and *smad9* not only share functional redundancy in early DV patterning but also are functionally exchangeable in regulating the differentiation of macrophages and granulocytes, both of which belong to the myeloid lineage.

## DISCUSSION

Smad1 and Smad5 are believed to be two major mediators transducing BMP signaling pathway, whereas BMP signals induce ventral fate in the early development of vertebrates (50). In zebrafish, the BMP ligands *bmp2b* and *bmp7* are widely expressed soon after the MBT, and then their expression becomes restricted to the ventral half of the embryo by the onset of gastrulation (51). It was believed that Smad1 and Smad5 should both play critical roles in DV patterning of zebrafish. In accordance with this, overexpression of either *smad1* or *smad5* in zebrafish embryos leads to ventralized phenotypes (Figs. 1 and 2) (9), similar to the phenotypic effects of *bmp2b* or *bmp4* overexpression (5). Overexpression of *smad1* in a different genetic background suggests that *smad1* is even more potent than *smad5* in promoting ventral fate. For instance, overexpression of *smad1* in a wild type background gives stronger ventralization than *smad5*, and *smad1* overexpression in a *smad5* mutant or *bmp2b* mutant leads to a rescue effect, whereas *smad5* overexpression cannot rescue the *bmp2b* mutant (9). However, from loss-of-function studies, we may even reach an opposite conclusion. Large scale mutation screens in zebrafish have identified several *smad5* mutants, such as *pgy* and *sbn*, which are strongly dorsalized (15), whereas no *smad1* mutant has been identified; effective knockdown of *smad1* expression by MO injection leads to no obvious defect on early DV patterning (Fig. 1*C*) (19). Here, we have revealed that a *smad1*-like gene, *smad9*, exists in the zebrafish genome, which could compensate for the Smad activity in the condition of *smad1* loss of function. We further prove that zebrafish *smad9* not only shows an expression pattern similar to that of *smad1* but also acts redundantly with *smad1* to mediate zebrafish DV patterning downstream of *smad5*.

It is proposed that the DV patterning in zebrafish can be divided into three distinct phases (17): an early Smad5- and Bmp2b-independent phase when an initial course of DV patterning is set up; an intermediate Smad5- and Bmp2b-dependent phase during which the initial DV patterning is refined and the morphogenetic Bmp2b gradient is established; and a later Smad5-independent phase after the onset of gastrulation when the Bmp2/4 gradient is interpreted. Direct evidence for this is the finding that the *smad5* mutant, *sbn*$^{-/-}$, can be rescued by *smad5* overexpression just after MBT, but there is no rescue effect if the exogenous *smad5* is strongly expressed during gastrulation and very weakly expressed at earlier stages (17). Our study suggests that the presence of Smad1 and Smad9 activities from 50% epiboly is the reason for the dispensability of Smad5 during gastrulation. The function of Smad5 during DV pattern-

ing is involved in setting up the putative morphogenetic BMP gradient along with other factors and, in addition, activates the expression of a cluster of genes, including *smad1* and *smad9*. From 50% epiboly, these two Smads interpret the BMP gradient during gastrulation in a redundant manner, and Smad1 and Smad9 become the executors of BMP/Smad in promoting ventral specification. In regard to the functional redundancy of *smad1* and *smad9*, if loss of function is utilized to study the relative roles of *smad1* and *smad9* in zebrafish DV patterning, we need to attenuate the activities of both of these two Smads in order to obtain informative results leading to precise conclusions.

The genetic regulation network and functional distinction of different BMP R-Smads in development are of great interest. It has been shown that Smad1 and Smad5 bind to different Smad-binding elements (SBEs) and activate different target genes (52–55). In different animal models, it is suggested that Smad1, Smad5, and Smad9 play different roles in various developmental processes. In chicken embryos, Smad9 is differently required during spinal cord neurogenesis compared with Smad1 and Smad5 (10). In *Smad1* mutant mice, the allantois fails to fuse to the chorion, with the result that they fail to connect to the placenta and die at ~10 days postcoitum (56, 57). *Smad5* mutant mice also die at about 10 postcoitum but for different reasons, including angiogenic failure, mesenchymal apoptosis, and other defects (58, 59). However, *Smad9* homozygous mutant mice develop normally and are viable and fertile (60). In the generation of dorsal spinal neural circuitry in mice, *Smad1* is required to regulate dl1 axon outgrowth, whereas *Smad5* is required for the generation of dorsal spinal neurons (61). In zebrafish, gene expression analysis revealed that *smad1* morphants and *smad5* morphants were deregulated for striking distinct genetic networks at the 1-somite stage (19). Our study reveals that *smad1* and *smad9* are two direct targets of *smad5*, that they start transcription prior the onset of gastrulation, and, more interestingly, that their transcription is negatively regulated by themselves and by each other (Fig. 5). The cross-regulated negative feedback loop between *smad1* and *smad9* and with themselves further supports the notion that *smad1* and *smad9* are redundant partners in regulating DV patterning because this phenomenon resembles the typical responsive circuit in the reciprocal regulation of redundant genes (45). In contrast, the upstream *smad5* is not affected by up- or down-regulation of *smad1* and *smad9*. Our results also suggest that the commonly known BMP targets, *szl* and *ved*, are probably the direct targets of *smad1* and *smad9* at the gastrula stage, instead of *smad5*, because their transcription is nearly abolished in *smad5*-overexpressed *smad1*/*smad9* double morphants (Fig. 4) (data not shown). We could even predicate that most BMP/Smad targets at the gastrula stage are probably the targets of BMP/Smad1/9. The functional redundancy of *smad1* and *smad9* is also hinted at by a previous study (62). For instance, zebrafish protein phosphatase 4c (Ppp4c) utilizes Smad1 as an adaptor to bind to the endogenous *id1* promoter, and depletion of both Smad1 and Smad9 activities could completely abolish this binding (62).

An interesting question is the mechanism of switching from Smad5 to Smad1 and Smad9 when gastrula begins. One possibility is that Smad1 and Smad9 can compete with Smad5 for interaction with Smad4, just as Smad3 competes with Smad2 for interacting with Smad4 and thus inhibits activin-induced goosecoid expression though Smad2/Smad4 (63). However, the ability of Smad5 to bind to Smad4 is not affected by the presence of an increasing amount of Smad1 or Smad9 (Fig. 6). Another possibility is that Smad1 and Smad9 rather than Smad5 are more potent activators for ventral promoting genes and BMP/Smad targets during gastrulation. The DNA element (GCAT) was previously characterized as the Smad1 SBE in the *Xvent-2B* (52) and *Xretpos* (53) promoters in *Xenopus* and in the *vegf* promoter in zebrafish (55). Several types of Smad5 SBEs were identified in different promoters, such as the DNA motif (GTCTAGAC) in the mouse *smad7* promoter (54) and the DNA motif (TGTCTGAGAC) in the zebrafish *vegf* (55) promoter. We have searched the upstream region of a BMP target gene, *szl*, for the DNA element identical to Smad1 SBE or Smad5 SBEs. Interestingly, 11 DNA elements identical to the Smad1 SBE (GCAT) but no DNA elements identical to Smad5 SBEs (GTCTAGAC or TGTCTGAGAC) were found in a 2000-bp DNA fragment upstream of the *szl* coding sequence. This suggests that *szl* is probably the direct target of Smad1 or Smad9 rather than Smad5. The other possibility is that these three Smads may bind to different cofactors. Previous studies have shown that B-cell translocation gene 2 (*Btg2*), a primary P53 transcriptional target gene, shows strong interaction with Smad1 and Smad9 but not with Smad5 (64), and Smad nuclear interacting protein 1 (SNIP1) only interacts with Smad1 (65).

The embryonic hematopoiesis depends on BMP/Smad signaling (66), whereas Smad1 and Smad5 differentially regulate this process (19). A previous study has revealed that *smad1* is required for the differentiation of the mature embryonic macrophages and granulocytes, whereas *smad5* is required for the primitive erythropoiesis. Because *smad1* and *smad9* show similar expression patterns during development and redundant function in DV patterning, it is reasonable that *smad9* is also involved in zebrafish hematopoiesis. In fact, myeloid defects are observed in embryos depleted for *smad9*, as in embryos depleted for *smad1*. Overexpression of *smad9* efficiently rescues the defects in *smad1* morphants and vice versa, and *smad5* is not able to rescue the myeloid defects in *smad1* or *smad9* morphants. In other words, *smad1* and *smad9* are exchangeable in regulating myelopoiesis, whereas *smad5* cannot replace them. Altogether, *smad1* and *smad9* not only share functional redundancy in regulating DV patterning but also have overlapping functions in myelopoiesis.

In conclusion, we have characterized the relative roles of *smad1*, *smad5*, and *smad9* during zebrafish DV patterning, and we have further revealed that *smad1* and *smad9* act redundantly to each other and function downstream of *smad5*. Therefore, our study has clearly clarified the regulation network and the cooperative roles of BMP R-Smads in early development of zebrafish.

*Acknowledgment—We thank Li Ming for fish husbandry.*

## REFERENCES


1. Massagué, J., and Wotton, D. (2000) Transcriptional control by the TGF-β/Smad signaling system. *EMBO J.* **19,** 1745–1754
2. Attisano, L., and Wrana, J. L. (2000) Smads as transcriptional co-modulators. *Curr. Opin. Cell Biol.* **12,** 235–243
3. Massagué, J. (1998) TGF-β signal transduction. *Annu. Rev. Biochem.* **67,** 753–791
4. Derynck, R., and Feng, X. H. (1997) TGF-β receptor signaling. *Biochim. Biophys. Acta* **1333,** F105–F150
5. Kishimoto, Y., Lee, K. H., Zon, L., Hammerschmidt, M., and Schulte-Merker, S. (1997) The molecular nature of zebrafish swirl. BMP2 function is essential during early dorsoventral patterning. *Development* **124,** 4457–4466
6. de Jong, J. L., and Zon, L. I. (2005) Use of the zebrafish system to study primitive and definitive hematopoiesis. *Annu. Rev. Genet.* **39,** 481–501
7. Graff, J. M., Bansal, A., and Melton, D. A. (1996) *Xenopus* Mad proteins transduce distinct subsets of signals for the TGF β superfamily. *Cell* **85,** 479–487
8. Suzuki, A., Chang, C., Yingling, J. M., Wang, X. F., and Hemmati-Brivanlou, A. (1997) Smad5 induces ventral fates in *Xenopus* embryo. *Dev. Biol.* **184,** 402–405
9. Dick, A., Meier, A., and Hammerschmidt, M. (1999) Smad1 and Smad5 have distinct roles during dorsoventral patterning of the zebrafish embryo. *Dev. Dyn.* **216,** 285–298
10. Le Dréau, G., Garcia-Campmany, L., Rabadán, M. A., Ferronha, T., Tozer, S., Briscoe, J., and Martí, E. (2012) Canonical BMP7 activity is required for the generation of discrete neuronal populations in the dorsal spinal cord. *Development* **139,** 259–268
11. Orvis, G. D., Jamin, S. P., Kwan, K. M., Mishina, Y., Kaartinen, V. M., Huang, S., Roberts, A. B., Umans, L., Huylebroeck, D., Zwijsen, A., Wang, D., Martin, J. F., and Behringer, R. R. (2008) Functional redundancy of TGF-β family type I receptors and receptor-Smads in mediating anti-Mullerian hormone-induced Mullerian duct regression in the mouse. *Biol. Reprod.* **78,** 994–1001
12. Wong, Y. L., Behringer, R. R., and Kwan, K. M. (2012) Smad1/Smad5 signaling in limb ectoderm functions redundantly and is required for interdigital programmed cell death. *Dev. Biol.* **363,** 247–257
13. Retting, K. N., Song, B., Yoon, B. S., and Lyons, K. M. (2009) BMP canonical Smad signaling through Smad1 and Smad5 is required for endochondral bone formation. *Development* **136,** 1093–1104
14. Pangas, S. A., Li, X., Umans, L., Zwijsen, A., Huylebroeck, D., Gutierrez, C., Wang, D., Martin, J. F., Jamin, S. P., Behringer, R. R., Robertson, E. J., and Matzuk, M. M. (2008) Conditional deletion of Smad1 and Smad5 in somatic cells of male and female gonads leads to metastatic tumor development in mice. *Mol. Cell. Biol.* **28,** 248–257
15. Haffter, P., Granato, M., Brand, M., Mullins, M. C., Hammerschmidt, M., Kane, D. A., Odenthal, J., van Eeden, F. J., Jiang, Y. J., Heisenberg, C. P., Kelsh, R. N., Furutani-Seiki, M., Vogelsang, E., Beuchle, D., Schach, U., Fabian, C., and Nüsslein-Volhard, C. (1996) The identification of genes with unique and essential functions in the development of the zebrafish, *Danio rerio*. *Development* **123,** 1–36
16. Lele, Z., Bakkers, J., and Hammerschmidt, M. (2001) Morpholino phenocopies of the swirl, snailhouse, somitabun, minifin, silberblick, and pipetail mutations. *Genesis* **30,** 190–194
17. Hild, M., Dick, A., Rauch, G. J., Meier, A., Bouwmeester, T., Haffter, P., and Hammerschmidt, M. (1999) The smad5 mutation somitabun blocks Bmp2b signaling during early dorsoventral patterning of the zebrafish embryo. *Development* **126,** 2149–2159
18. Kramer, C., Mayr, T., Nowak, M., Schumacher, J., Runke, G., Bauer, H., Wagner, D. S., Schmid, B., Imai, Y., Talbot, W. S., Mullins, M. C., and Hammerschmidt, M. (2002) Maternally supplied Smad5 is required for ventral specification in zebrafish embryos prior to zygotic Bmp signaling. *Dev. Biol.* **250,** 263–279
19. McReynolds, L. J., Gupta, S., Figueroa, M. E., Mullins, M. C., and Evans, T. (2007) Smad1 and Smad5 differentially regulate embryonic hematopoiesis. *Blood* **110,** 3881–3890
20. Dee, C. T., Gibson, A., Rengifo, A., Sun, S. K., Patient, R. K., and Scotting, P. J. (2007) A change in response to Bmp signalling precedes ectodermal fate choice. *Int. J. Dev. Biol.* **51,** 79–84
21. Westerfield, M. (2000) *The Zebrafish Book: A Guide for the Laboratory Use of Zebrafish (Danio rerio)*, 4th Ed., University of Oregon Press, Eugene, OR
22. Kimmel, C. B., Ballard, W. W., Kimmel, S. R., Ullmann, B., and Schilling, T. F. (1995) Stages of embryonic development of the zebrafish. *Dev. Dyn.* **203,** 253–310
23. Chen, C. H., Sun, Y. H., Pei, D. S., and Zhu, Z. Y. (2009) Comparative expression of zebrafish lats1 and lats2 and their implication in gastrulation movements. *Dev. Dyn.* **238,** 2850–2859
24. Nordnes, S., Krauss, S., and Johansen, T. (1994) cDNA sequence of zebrafish (*Brachydanio rerio*) translation elongation factor-1 α. Molecular phylogeny of eukaryotes based on elongation factor-1 α protein sequences. *Biochim. Biophys. Acta* **1219,** 529–532
25. Keegan, B. R., Feldman, J. L., Lee, D. H., Koos, D. S., Ho, R. K., Stainier, D. Y., and Yelon, D. (2002) The elongation factors Pandora/Spt6 and Foggy/Spt5 promote transcription in the zebrafish embryo. *Development* **129,** 1623–1632
26. Alcaraz-Pérez, F., Mulero, V., and Cayuela, M. L. (2008) Application of the dual-luciferase reporter assay to the analysis of promoter activity in zebrafish embryos. *BMC Biotechnol.* **8,** 81
27. Liu, Y., Bourgeois, C. F., Pang, S., Kudla, M., Dreumont, N., Kister, L., Sun, Y. H., Stevenin, J., and Elliott, D. J. (2009) The germ cell nuclear proteins hnRNP G-T and RBMY activate a testis-specific exon. *PLoS Genet.* **5,** e1000707
28. Poulain, M., and Lepage, T. (2002) Mezzo, a paired-like homeobox protein is an immediate target of Nodal signalling and regulates endoderm specification in zebrafish. *Development* **129,** 4901–4914
29. Thisse, B., Heyer, V., Lux, A., Alunni, V., Degrave, A., Seiliez, I., Kirchner, J., Parkhill, J. P., and Thisse, C. (2004) Spatial and temporal expression of the zebrafish genome by large-scale *in situ* hybridization screening. *Methods Cell Biol.* **77,** 505–519
30. Kudoh, T., Tsang, M., Hukriede, N. A., Chen, X., Dedekian, M., Clarke, C. J., Kiang, A., Schultz, S., Epstein, J. A., Toyama, R., and Dawid, I. B. (2001) A gene expression screen in zebrafish embryogenesis. *Genome Res.* **11,** 1979–1987
31. Rhinn, M., Lun, K., Luz, M., Werner, M., and Brand, M. (2005) Positioning of the midbrain-hindbrain boundary organizer through global posteriorization of the neuroectoderm mediated by Wnt8 signaling. *Development* **132,** 1261–1272
32. Yabe, T., Shimizu, T., Muraoka, O., Bae, Y. K., Hirata, T., Nojima, H., Kawakami, A., Hirano, T., and Hibi, M. (2003) Ogon/Secreted Frizzled functions as a negative feedback regulator of Bmp signaling. *Development* **130,** 2705–2716
33. Gilardelli, C. N., Pozzoli, O., Sordino, P., Matassi, G., and Cotelli, F. (2004) Functional and hierarchical interactions among zebrafish vox/vent homeobox genes. *Dev. Dyn.* **230,** 494–508
34. Wang, H., Long, Q., Marty, S. D., Sassa, S., and Lin, S. (1998) A zebrafish model for hepatoerythropoietic porphyria. *Nat. Genet.* **20,** 239–243
35. Herbomel, P., Thisse, B., and Thisse, C. (1999) Ontogeny and behaviour of early macrophages in the zebrafish embryo. *Development* **126,** 3735–3745
36. Bennett, C. M., Kanki, J. P., Rhodes, J., Liu, T. X., Paw, B. H., Kieran, M. W., Langenau, D. M., Delahaye-Brown, A., Zon, L. I., Fleming, M. D., and Look, A. T. (2001) Myelopoiesis in the zebrafish, *Danio rerio*. *Blood* **98,** 643–651
37. Liu, Z., Lin, X., Cai, Z., Zhang, Z., Han, C., Jia, S., Meng, A., and Wang, Q. (2011) Global identification of SMAD2 target genes reveals a role for multiple co-regulatory factors in zebrafish early gastrulas. *J. Biol. Chem.* **286,** 28520–28532
38. Belting, H. G., Wendik, B., Lunde, K., Leichsenring, M., Mössner, R., Driever, W., and Onichtchouk, D. (2011) Pou5f1 contributes to dorsoventral patterning by positive regulation of vox and modulation of fgf8a expression. *Dev. Biol.* **356,** 323–336
39. Wang, L., Liu, Y. T., Hao, R., Chen, L., Chang, Z., Wang, H. R., Wang, Z. X., and Wu, J. W. (2011) Molecular mechanism of the negative regulation of Smad1/5 by CHIP. *J. Biol. Chem.* **286,** 15883–15894
40. Müller, F., Blader, P., Rastegar, S., Fischer, N., Knöchel, W., and Strähle, U. (1999) Characterization of zebrafish smad1, smad2 and smad5. The ami-

no-terminus of smad1 and smad5 is required for specific function in the embryo. *Mech. Dev.* **88,** 73–88
41. Hammerschmidt, M., Serbedzija, G. N., and McMahon, A. P. (1996) Genetic analysis of dorsoventral pattern formation in the zebrafish. Requirement of a BMP-like ventralizing activity and its dorsal repressor. *Genes Dev.* **10,** 2452–2461
42. Mullins, M. C., Hammerschmidt, M., Kane, D. A., Odenthal, J., Brand, M., van Eeden, F. J., Furutani-Seiki, M., Granato, M., Haffter, P., Heisenberg, C. P., Jiang, Y. J., Kelsh, R. N., and Nüsslein-Volhard, C. (1996) Genes establishing dorsoventral pattern formation in the zebrafish embryo. The ventral specifying genes. *Development* **123,** 81–93
43. Chen, D., Zhao, M., and Mundy, G. R. (2004) Bone morphogenetic proteins. *Growth Factors* **22,** 233–241
44. Eisen, J. S., and Smith, J. C. (2008) Controlling morpholino experiments. Don't stop making antisense. *Development* **135,** 1735–1743
45. Kafri, R., Springer, M., and Pilpel, Y. (2009) Genetic redundancy. New tricks for old genes. *Cell* **136,** 389–392
46. Maéno, M., Ong, R. C., Suzuki, A., Ueno, N., and Kung, H. F. (1994) A truncated bone morphogenetic protein 4 receptor alters the fate of ventral mesoderm to dorsal mesoderm. Roles of animal pole tissue in the development of ventral mesoderm. *Proc. Natl. Acad. Sci. U.S.A.* **91,** 10260–10264
47. Xu, C., Fan, Z. P., Müller, P., Fogley, R., DiBiase, A., Trompouki, E., Unternaehrer, J., Xiong, F., Torregroza, I., Evans, T., Megason, S. G., Daley, G. Q., Schier, A. F., Young, R. A., and Zon, L. I. (2012) Nanog-like regulates endoderm formation through the Mxtx2-Nodal pathway. *Dev. Cell* **22,** 625–638
48. Whitman, M., and Raftery, L. (2005) TGF$\beta$ signaling at the summit. *Development* **132,** 4205–4210
49. Feng, X. H., and Derynck, R. (2005) Specificity and versatility in TGF-$\beta$ signaling through Smads. *Annu. Rev. Cell Dev. Biol.* **21,** 659–693
50. von Bubnoff, A., and Cho, K. W. (2001) Intracellular BMP signaling regulation in vertebrates. Pathway or network? *Dev. Biol.* **239,** 1–14
51. Schier, A. F., and Talbot, W. S. (2005) Molecular genetics of axis formation in zebrafish. *Annu. Rev. Genet.* **39,** 561–613
52. Henningfeld, K. A., Friedle, H., Rastegar, S., and Knöchel, W. (2002) Autoregulation of Xvent-2B. Direct interaction and functional cooperation of Xvent-2 and Smad1. *J. Biol. Chem.* **277,** 2097–2103
53. Shima, D. T., Kuroki, M., Deutsch, U., Ng, Y. S., Adamis, A. P., and D'Amore, P. A. (1996) The mouse gene for vascular endothelial growth factor. Genomic structure, definition of the transcriptional unit, and characterization of transcriptional and post-transcriptional regulatory sequences. *J. Biol. Chem.* **271,** 3877–3883
54. Li, W., Chen, F., Nagarajan, R. P., Liu, X., and Chen, Y. (2001) Characterization of the DNA-binding property of Smad5. *Biochem. Biophys. Res. Commun.* **286,** 1163–1169
55. He, C., and Chen, X. (2005) Transcription regulation of the vegf gene by the BMP/Smad pathway in the angioblast of zebrafish embryos. *Biochem. Biophys. Res. Commun.* **329,** 324–330
56. Tremblay, K. D., Dunn, N. R., and Robertson, E. J. (2001) Mouse embryos lacking Smad1 signals display defects in extra-embryonic tissues and germ cell formation. *Development* **128,** 3609–3621
57. Lechleider, R. J., Ryan, J. L., Garrett, L., Eng, C., Deng, C., Wynshaw-Boris, A., and Roberts, A. B. (2001) Targeted mutagenesis of Smad1 reveals an essential role in chorioallantoic fusion. *Dev. Biol.* **240,** 157–167
58. Chang, H., Huylebroeck, D., Verschueren, K., Guo, Q., Matzuk, M. M., and Zwijsen, A. (1999) Smad5 knockout mice die at mid-gestation due to multiple embryonic and extraembryonic defects. *Development* **126,** 1631–1642
59. Yang, X., Castilla, L. H., Xu, X., Li, C., Gotay, J., Weinstein, M., Liu, P. P., and Deng, C. X. (1999) Angiogenesis defects and mesenchymal apoptosis in mice lacking SMAD5. *Development* **126,** 1571–1580
60. Arnold, S. J., Maretto, S., Islam, A., Bikoff, E. K., and Robertson, E. J. (2006) Dose-dependent Smad1, Smad5, and Smad8 signaling in the early mouse embryo. *Dev. Biol.* **296,** 104–118
61. Hazen, V. M., Andrews, M. G., Umans, L., Crenshaw, E. B., 3rd, Zwijsen, A., and Butler, S. J. (2012) BMP receptor-activated Smads confer diverse functions during the development of the dorsal spinal cord. *Dev. Biol.* **367,** 216–227
62. Jia, S., Dai, F., Wu, D., Lin, X., Xing, C., Xue, Y., Wang, Y., Xiao, M., Wu, W., Feng, X. H., and Meng, A. (2012) Protein phosphatase 4 cooperates with Smads to promote BMP signaling in dorsoventral patterning of zebrafish embryos. *Dev. Cell* **22,** 1065–1078
63. Labbé, E., Silvestri, C., Hoodless, P. A., Wrana, J. L., and Attisano, L. (1998) Smad2 and Smad3 positively and negatively regulate TGF$\beta$-dependent transcription through the forkhead DNA-binding protein FAST2. *Mol. Cell* **2,** 109–120
64. Park, S., Lee, Y. J., Lee, H. J., Seki, T., Hong, K. H., Park, J., Beppu, H., Lim, I. K., Yoon, J. W., Li, E., Kim, S. J., and Oh, S. P. (2004) B-cell translocation gene 2 (Btg2) regulates vertebral patterning by modulating bone morphogenetic protein/smad signaling. *Mol. Cell Biol.* **24,** 10256–10262
65. Kim, R. H., Wang, D., Tsang, M., Martin, J., Huff, C., de Caestecker, M. P., Parks, W. T., Meng, X., Lechleider, R. J., Wang, T., and Roberts, A. B. (2000) A novel smad nuclear interacting protein, SNIP1, suppresses p300-dependent TGF-$\beta$ signal transduction. *Genes Dev.* **14,** 1605–1616
66. Schmerer, M., and Evans, T. (2003) Primitive erythropoiesis is regulated by Smad-dependent signaling in postgastrulation mesoderm. *Blood* **102,** 3196–3205